Contacts Between Alcohols in Water are Random Rather than Hydrophobic

Blake M. Rankin[1], Dor Ben-Amotz[1], Sietse T. van der Post[2], and Huib J. Bakker[2]*

(1) Purdue University, Department of Chemistry, West Lafayette, IN 47907, USA.

(2) FOM Institute AMOLF, Science Park 104, 1098 XG Amsterdam, The Netherlands.

AUTHOR INFORMATION

Corresponding Author

*Email: bendor@purdue.edu

Abstract. Given the presumed importance of water-mediated hydrophobic interactions in a wide range of biological and synthetic self-assembly processes, it is remarkable that both the sign and the magnitude of the hydrophobic interactions between simple amphiphiles, such as alcohols, remain unresolved. To address this question, we have performed Raman hydration-shell vibrational spectroscopy and polarization-resolved femtosecond infrared experiments, as well as random mixing and molecular dynamics simulations. Our results indicate that there are no more hydrophobic contacts in aqueous solutions of alcohols ranging from methanol to tertiary butyl alcohol than in random mixtures of the same concentration. This implies that the interaction between small hydrophobic groups is weaker than thermal energy fluctuations. Thus, the corresponding water-mediated hydrophobic interaction must be repulsive, with a magnitude sufficient to negate the attractive direct van der Waals interaction between the hydrophobic groups.

TOC GRAPHIC

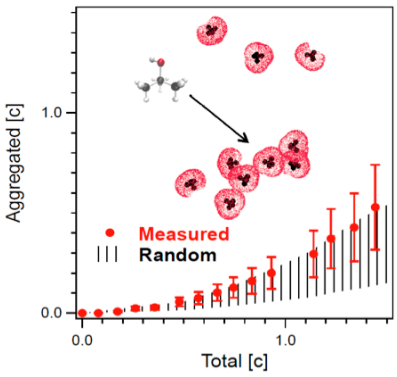

KEYWORDS

Raman spectroscopy, femtosecond IR spectroscopy, hydrophobic interactions, random mixing

The hydrophobic aversion of oil for water is considered to play a central role in the self-assembly of a wide variety of biological structures and devices.[1-6] More specifically, the mean force potential associated with the interactions between molecules dissolved in water may in general be represented as the sum of direct and water-mediated interactions. Direct interactions are those between the isolated molecules (in the absence of water) while water-mediated interactions reflect the additional influence of water in either promoting or suppressing aggregation. For idealized hydrophobic hard-sphere solutes, the water-mediated interaction is predicted to be *attractive* with a magnitude of the order of *RT*, which increases with solute size.[5, 7] However, for real hydrophobic molecules, such as methane, the water-mediated interaction is predicted to be much weaker,[7-9] and for larger molecules such as neopentane, adamantane, and C_{60}, this interaction has even been predicted to become increasingly *repulsive* with increasing solute size.[10-11] However, such theoretical predictions of the hydrophobic interaction are quite sensitive to assumptions made in performing either classical[9-13] or quantum[14] molecular dynamics (MD) simulations. Thus, the magnitude (and even sign) of the hydrophobic interaction remains a subject of theoretical debate, and has yet to be experimentally determined.

Aqueous tertiary butyl alcohol (TBA) solutions provide an appealing model system for investigating hydrophobic interactions, and have been studied using neutron,[15] x-ray,[16] and light[17] scattering, infrared,[18] Raman,[19-20] Brillouin,[21] and NMR[22] spectroscopy, mass spectrometry,[23] and thermodynamic[24-27] methods, as well as MD[12] and integral equation[28] calculations (see also references therein). Although previous studies generally agree that there is little TBA aggregation below a concentration of ~1 M (which corresponds to a TBA mole fraction of $\chi \sim 0.02$), it remains unclear whether or not the observed aggregation is the result of attractive hydrophobic interactions, or rather the result of random contacts. Here we significantly extend a

preliminary investigation of this question[29] by combining polarization-resolved femtosecond infrared (fs-IR) and Raman multivariate curve resolution (Raman-MCR) measurements to establish self-consistent bounds on the number of direct hydrophobic contacts in dilute aqueous TBA solutions, and quantitatively compare the results with both random mixing (RM) and MD simulation predictions. To test the generality of our conclusions we have performed additional Raman-MCR and MD studies of aqueous methanol and n-butanol solutions. In the remainder of the paper, we describe results indicating that the mean force potential between small hydrocarbon groups in water is smaller than the direct interaction energy between the hydrocarbon groups – thus indicating that the corresponding water-mediated interaction is repulsive, so it drives the hydrocarbon groups apart rather than pulling them closer together.

Figure 1A shows the experimentally measured fraction of slow water molecules in aqueous TBA solutions, obtained from fs-IR decay curves (some examples of which are shown in the inset panel). The measured fs-IR decay curves are fit to bi-exponential functions to obtain the fraction f of the total number of water molecules whose reorientation times are significantly slower (> 2.5 ps) than bulk water.[30] The fact that f depends linearly on TBA concentration below ~1 M implies that there is little TBA aggregation in this concentration range. The data in fact closely follow the RM prediction $f = 1 - e^{-\alpha[TBA]}$ (dashed curve) pertaining to a system with a uniform TBA concentration (as further described in the Supplementary Information). The value of $\alpha \sim 0.15$ L/mol, obtained from the initial slope of the experimental points in Figure 1A, represents the volume of the hydrophobic hydration-shell of TBA.

The Raman-MCR hydration-shell spectra shown in the inset of Figure 1B were obtained by using self-modeling curve resolution (SMCR)[31-32] to extract TBA solute-correlated (SC) spectra from pairs of measured spectra (one from pure water and the other from a TBA solution).

The resulting SC spectra indicate how the OH stretch band arising from the hydration-shell of TBA differs from bulk water. The SC OH spectra shown in Figure 1B are each normalized to the corresponding CH stretch band area of TBA, and thus reveal how the hydration-shell around each TBA molecule changes with TBA concentration (with little or no contribution from the OH head group of TBA).[29, 32] More specifically, the hydration-shell OH bands shown in Figure 1B include contributions from H-bonded hydration-shell water molecules (between ~3100 cm^{-1} and 3750 cm^{-1}) and a small water dangling OH peak (at ~3660 cm^{-1}).[33] The decrease in the SC OH area with increasing TBA concentration implies that the average number of perturbed (not bulk-like) water molecules around each TBA decreases with increasing TBA concentration.

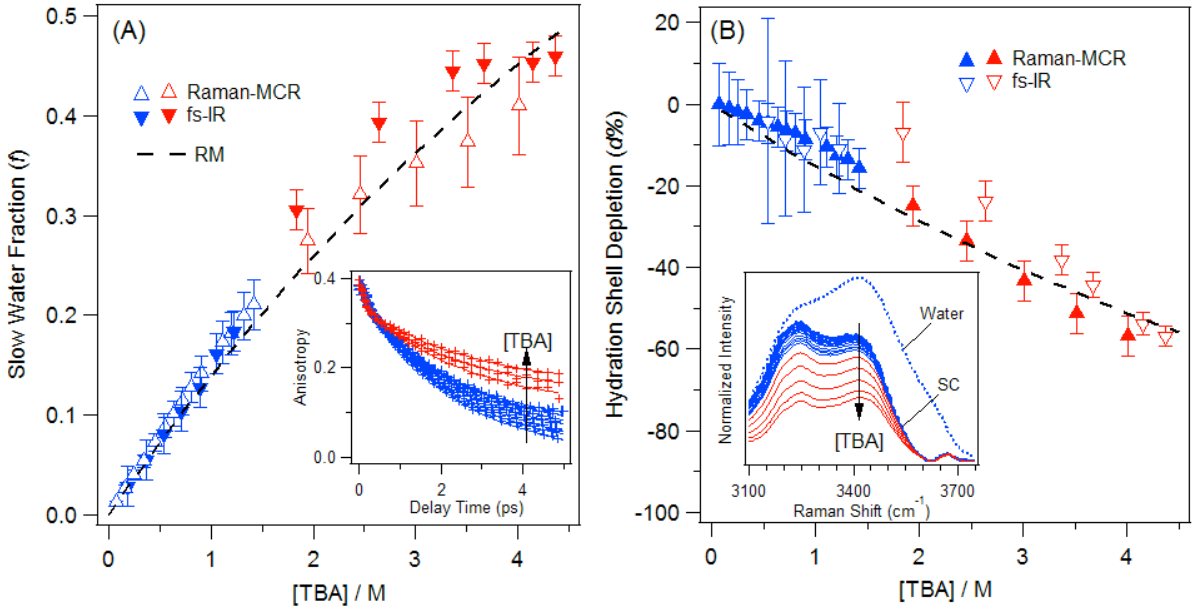

Figure 1. (A) fs-IR decay curves from which the slow water fractions (solid points) were obtained. (B) OH Raman band of pure water (dotted blue curve) and the Raman-MCR SC spectra (normalized to the TBA CH area) from which the hydration-shell depletion percentages (solid points) were obtained. The open points were obtained using Eq. 1. The black dashed curves correspond to RM predictions. The error bars on the solid points represent experimental

standard deviations while those on the open points pertain to using $n_0 = 8.3 \pm 1$ in Eq. 1. A small non-zero intercept (equal to ~0.01) has been subtracted from all of the fs-IR f values.

If we identify n_0 as the number of slow water molecule around an isolated (dilute) TBA and n as the average number of slow waters per TBA at some higher concentration, then we can convert the fs-IR slow water fraction f (solid points in Figure 1A) to the corresponding hydration-shell depletion percentage $d\%$ using the following expression (with no adjustable parameters),

$$d\% = 100\left(\frac{n - n_0}{n_0}\right) = 100\left(\frac{f}{n_0}\frac{N_W}{N_S} - 1\right) \qquad (1)$$

Note that $n = f\,(N_W/N_S) = f(1/\chi - 1)$, where N_W/N_S is the ratio of the number of water and solute (TBA) molecules in a given solution, and $n_0 = \alpha\,[H_2O] \approx \alpha\,(M^{-1})\ 55.5\ (M) \approx 8.3 \pm 1$, where $\alpha = df/d[TBA] \approx 0.15$ L/mol is the initial slope of the experimental fs-IR points in Figure 1A. The variables n, f, N_W, and N_S all depend on TBA concentration while n_0 is a constant. The $d\%$ values obtained from the fs-IR f values (solid points in Figure 1A) are indicated by the open points in Figure 1B. Conversely, we may use Eq. 1 to convert the Raman-MCR $d\%$ values (solid points in Figure 1B) to f values using the experimentally determined value of $n_0 = 8.3$. The resulting f values are indicated by the open points in Figure 1A. The agreement between the $d\%$ and f results (open and closed points in both panels of Figure 1) obtained using two quite different experimental methods implies that the water molecules whose OH spectra are perturbed by TBA are the same water molecules whose reorientation times are significantly longer than bulk water. Moreover, the agreement between the random mixing predictions (dashed curve) and the Raman-MCR $d\%$ results in Figure 1B implies that the observed hydration shell depletion is

the result of random, not hydrophobic, contacts between TBA molecules, as further quantified below.

The results shown in Figure 2 compare the concentrations of monomeric and aggregated alcohol molecules in aqueous solutions of TBA, methanol, and n-butanol (points), as well as the corresponding RM predictions (shaded regions and dashed curves). The monomer and aggregate hydration shell spectra shown in the inset panel of Figure 2A were obtained by applying a second round of SMCR to the hydration-shell spectra shown in Figure 1B. The bounds on the aggregate hydration-shell spectra and error bars on the experimental points arise from the mathematical "rotational ambiguity" of the SMCR spectral decomposition[29, 34] (as further explained in Supplementary Information). The numerical RM predictions shown in Figure 2 were obtained from the average number of monomeric TBA molecules (with no intermolecular methyl-methyl contacts) in random mixtures of alcohols (as further described in the Supplementary Information). The dashed curves in Figure 2A represent RM predictions obtained assuming a hydration shell volume of 0.15 L/mol, determined from the initial slope of f vs [TBA] in Figure 1B. The shaded regions in Figure 2 represent the range of RM predictions obtained using independent methyl-methyl coordination shell volume estimates based on either the first peak or first minimum of the methyl-methyl radial distribution of aqueous TBA (see Supplementary Information).

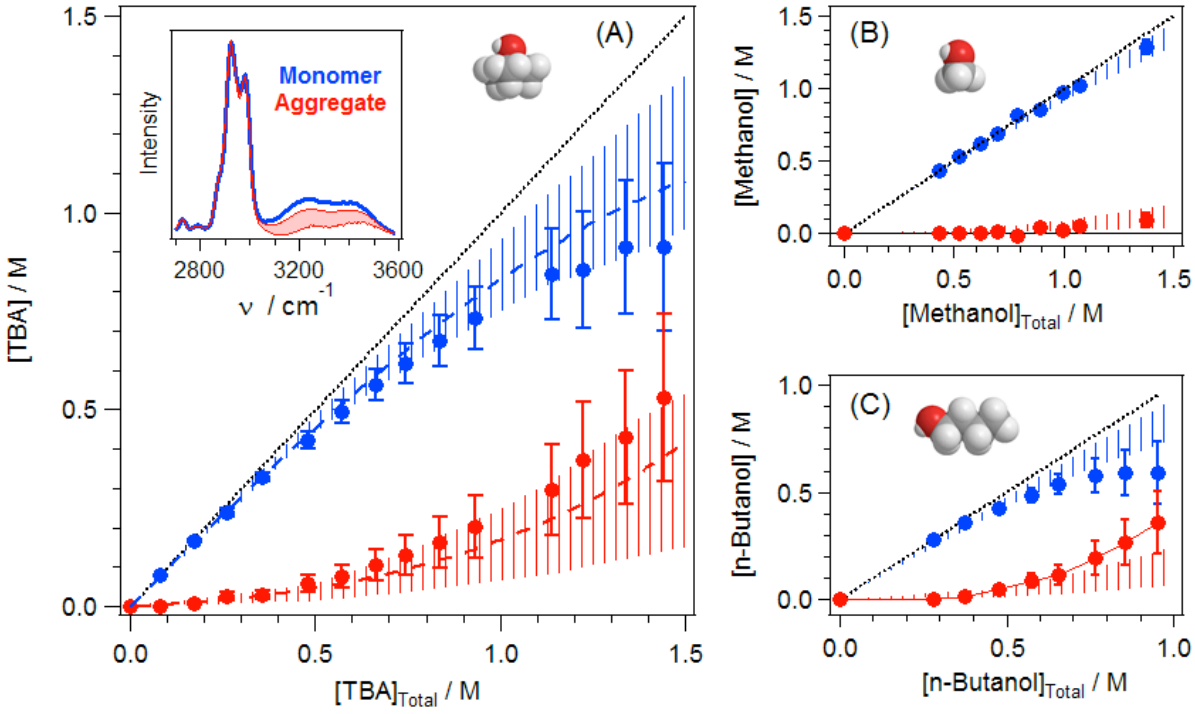

Figure 2. Concentrations of monomers (blue) and aggregated (red) alcohols in aqueous solutions of (A) TBA, (B) methanol, and (C) n-butanol obtained from Raman-MCR (points) and RM predictions (shaded regions).The inset panel in (A) shows the corresponding hydration-shell OH stretch components, including upper and lower bounds on the aggregate hydration-shell spectrum. The error bars on the experimental points are determined by the latter bounds. The dashed RM prediction curves are obtained assuming a hydrophobic hydration-shell volume α~0.15 L/mol, consistent with the initial slope of f vs [TBA] in Figure 1A, and the shaded regions correspond to RM predictions obtained assuming independently determined bounds on the methyl-methyl coordination shell volume (see Supplementary Information).

The agreement between the experimental and RM results in Figure 2 confirm that contacts between alcohols in water are indeed approximately random. Moreover, the methanol and n-butanol results shown Figures 2B and 3C indicate that our conclusion is general, as it

applies to aqueous solutions containing other small alcohols. More quantitatively, the very small difference between the experimental (points) and RM (dashed curve) concentrations of aggregated TBA molecules at a TBA concentration of 1 M imply that the contact value of the mean force potential is approximately $\Delta G = -RT \ln(0.23/0.18) \sim -0.6\pm2$ kJ/mol, which is small compared to ambient thermal energy fluctuations ($RT \sim 2.5$ kJ/mol). To put this result in perspective, note that the direct interaction energy between two methane molecules (in the absence of water) has an attractive well depth of ~1.2 kJ/mol[9] while that between larger alkanes increases approximately linearly with the number of carbons (with a slope of ~0.6 kJ/mol per carbon[35]), and thus a butyl group is predicted to have a direct interaction well of about 3 kJ/mol. Moreover, MD simulations have predicted that neopentane molecules have a direct interaction well depth of ~8±5 kJ/mol.[10-11] Thus, the fact that the latter direct interaction well depth estimates are larger than our experimentally derived mean force potential well depth 0.6±2 kJ/mol clearly implies that the water-mediated hydrophobic interaction between TBA hydrocarbon groups must be *repulsive* with a magnitude sufficient to largely negate the *attractive* direct van der Waals interaction between TBA molecules.

It is also noteworthy that classical MD simulations of a 1 M aqueous TBA solution (using OPLS-AA/TIP4P potentials) yield an attractive contact mean force potential of -2.8±1 kJ/mol (see Supplementary Information), thus indicating that such simulation slightly overestimate the total hydrophobic interaction free energy. However, since 2.8 kJ/mol is slightly smaller than the estimated direct attractive interaction well depth between butyl groups or neopentane molecules, our simulation results may nevertheless be consistent with our conclusion that the corresponding water-mediated interaction is slightly repulsive.

It is also interesting to note that our conclusions are apparently consistent with previous thermodynamic excess hydration enthalpy[26, 36] and osmotic second virial coefficient[24, 27] results that have been interpreted as indicating that water-mediated interaction between small alcohols are repulsive. However, such thermodynamic measurements cannot in themselves be used to quantify the number of direct contacts between solutes or to determine the associated water-mediated contact free energy (without additional input from simulations or other kinds of experiments).

Our results imply that the interaction free energy (mean force potential) between hydrophobic groups is relatively insensitive hydrocarbon chain branching and water nuclear quantum effects. More specifically, we have found that the two butanol isomer (see Figures 2A and 2C) have quite similar nearly random mixing behavior (up to the ~1 M solubility limit of n-butanol). In other words, the free energy difference between butanol monomers and the initially formed hydrophobic contact aggregates is relatively insensitive to the branching structure of the hydrophobic group, while the much lower solubility of n-butanol than TBA (which is infinitely miscible in water) implies that the free energy of the corresponding pure alcohols is quite sensitive to chain branching. We have also performed Raman-MCR measurements of aqueous TBA solutions in D_2O and found no detectable difference between the degree of TBA aggregation in D_2O and H_2O (see Supplementary Information), thus revealing that aggregation is not sensitive to nuclear quantum effects (which are responsible for the stronger hydrogen bonding in D_2O than H_2O).

Our finding that hydrophobic interactions between alcohol molecules are too weak to provide a significant driving force for aggregation appears to contrast with other observations, such as the immiscibility of oil and water and the decrease in critical micelle concentrations with

increasing surfactant chain length. The solution to this paradox is that the strength of the hydrophobic interaction strongly depends on hydrophobic contact surface area. Our results imply that the water network accommodates small hydrophobic solutes quite well, thus making the water-mediated interaction repulsive and the net driving force for forming a single direct methyl-methyl contact negligibly small. However, hydrophobic interactions are expected to become increasingly favorable when transferring a non-polar group into aggregates containing multiple hydrophobic molecules[30, 37-39] or into a protein's hydrophobic binding pocket.[2] Thus, mounting evidence suggests that hydrophobic interactions only exceed random thermal energy fluctuations when more than approximately 1 nm^2 of solvent accessible hydrophobic surface area is removed from water.

Experimental Methods

Raman-MCR. Methanol (High Purity Solvent, OmniSolv), n-butanol (99.8 %, Sigma Aldrich), and tert-butyl alcohol (≥99.5% TBA, Sigma Aldrich) were used without further purification. Aqueous solutions ranging in concentration from 0 to 4 M (for methanol and TBA) and 0 to 1 M (for n-butanol) were prepared using ultra-pure water (Milli-Q UF Plus, 18.2 mΩ·cm resistance, Millipore). For the deuterated experiments, d9-TBA (98%, Cambridge Isotope Laboratories) and D2O (99.9%, Cambridge Isotope Laboratories) were used. Spectra were collected with an integration time of 0.2 seconds and a total scan time of five minutes per spectrum (between two and four replicates each). The same custom-built Raman spectroscopic instrument was used as previously described[32-33]. The Self-Modeling Curve Resolution (SMCR) [31-32, 34] analysis strategy to obtain the results in Figure 1 is further described and illustrated in the Supplementary Information.

fs-IR. We measure the reorientation dynamics of HDO molecules in aqueous solutions of tertiary-butyl alcohol (≥99.5%, Sigma Aldrich). The water solvent is prepared by adding 4% heavy water D_2O to H_2O, leading to a solution of 8% HDO in H_2O. The reorientation dynamics of the OD groups are measured with polarization-resolved pump-probe spectroscopy. The pulses used in this experiment have pulse energies of ~5 μJ, a pulse duration of 120 fs and a central wavelength of 4 μm. The pump pulse excites the OD stretch vibration of a few percent of the HDO molecules. This excitation is anisotropic because of the preferential excitation of HDO molecules that have their OD groups oriented parallel to the pump polarization. The anisotropy of the excitation is probed with two time-delayed probe pulses that are polarized parallel and perpendicular to the pump polarization. With increasing delay time, the anisotropy decays due to reorientation of the water molecules.

ASSOCIATED CONTENT

Supporting Information. Additional experimental and simulation details and results. This material is available free of charge via the Internet at http://pubs.acs.org.

AUTHOR INFORMATION

Corresponding Author

*Email: bendor@purdue.edu

Notes

The authors declare no competing financial interests.

ACKNOWLEDGMENT

B.M.R. and D.B.A acknowledge financial support for this work from the National Science Foundation (CHE-1213338) and a PRF Research Grant from Purdue University. The work by S.T.P and H.J.B is part of the research program of the "Stichting voor Fundamenteel Onderzoek der Materie (FOM)", which is financially supported by the ''Nederlandse organisatie voor Wetenschappelijk Onderzoek (NWO)." The authors also acknowledge Yuan Yuan for the density measurements (see Supplementary Information) and Rini Gupta and G.N. Patey for useful discussions and sharing the large-scale MD simulations of aqueous TBA solutions.

REFERENCES

1. Patel, A. J.; Varilly, P.; Jamadagni, S. N.; Hagan, M. F.; Chandler, D.; Garde, S. Sitting at the Edge: How Biomolecules Use Hydrophobicity to Tune Their Interactions and Function. *J. Phys. Chem. B* **2012,** *116*, 2498-2503.

2. Hummer, G. Molecular Binding under Water's Influence. *Nat. Chem.* **2010,** *2*, 906-907.

3. Rasaiah, J. C.; Garde, S.; Hummer, G. Water in Nonpolar Confinement: From Nanotubes to Proteins and Beyond. *Annu. Rev. Phys. Chem.* **2008,** *59*, 713-740.

4. Granick, S.; Bae, S. C. A Curious Antipathy for Water. *Science* **2008,** *322*, 1477-1478.

5. Chandler, D. Interfaces and the Driving Force of Hydrophobic Assembly. *Nature* **2005,** *437*, 640-647.

6. Baldwin, R. L. Dynamic Hydration Shell Restores Kauzmann's 1959 Explanation of How the Hydrophobic Factor Drives Protein Folding. *Proc. Natl. Acad. Sci. U. S. A.* **2014,** *111*, 13052-13056.

7. Ben-Naim, A. *Hydrophobic Interactions*. Plenum Press: New York, 1980.

8. Pratt, L. R.; Chandler, D. Hydrophobic Interactions and Osmotic 2nd Virial-Coefficients for Methanol in Water. *J. Solut. Chem.* **1980,** *9*, 1-17.

9. Koga, K. Osmotic Second Virial Coefficient of Methane in Water. *J. Phys. Chem. B* **2013,** *117*, 12619-12624.

10. Morrone, J. A.; Li, J.; Berne, B. J. Interplay between Hydrodynamics and the Free Energy Surface in the Assembly of Nanoscale Hydrophobes. *J. Phys. Chem. B* **2012,** *116*, 378-389.

11. Makowski, M.; Czaplewski, C.; Liwo, A.; Scheraga, H. A. Potential of Mean Force of Association of Large Hydrophobic Particles: Toward the Nanoscale Limit. *J. Phys. Chem. B* **2010,** *114*, 993-1003.

12. Gupta, R.; Patey, G. N. Aggregation in Dilute Aqueous Tert-Butyl Alcohol Solutions: Insights from Large-Scale Simulations. *J. Chem. Phys.* **2012,** *137*, 034509.

13. Ghosh, M. K.; Uddin, N.; Choi, C. H. Hydrophobic and Hydrophilic Associations of a Methanol Pair in Aqueous Solution. *J. Phys. Chem. B* **2012,** *116*, 14254-14260.

14. Li, J. L.; Car, R.; Tang, C.; Wingreen, N. S. Hydrophobic Interaction and Hydrogen-Bond Network for a Methane Pair in Liquid Water. *Proc. Natl. Acad. Sci. U. S. A.* **2007,** *104*, 2626-2630.

15. Bowron, D. T.; Finney, J. L. Anion Bridges Drive Salting out of a Simple Amphiphile from Aqueous Solution. *Phys. Rev. Lett.* **2002,** *89*, 215508.

16. Nishikawa, K.; Hayashi, H.; Iijima, T. Temperature-Dependence of the Concentration Fluctuation, the Kirkwood-Buff Parameters, and the Correlation Length of Tert-Butyl Alcohol and Water Mixtures Studied by Small-Angle X-Ray-Scattering. *J. Phys. Chem.* **1989,** *93*, 6559-6565.

17. Sedlak, M.; Rak, D. Large-Scale Inhomogeneities in Solutions of Low Molar Mass Compounds and Mixtures of Liquids: Supramolecular Structures or Nanobubbles? *J. Phys. Chem. B* **2013,** *117*, 2495-2504.

18. Petersen, C.; Bakulin, A. A.; Pavelyev, V. G.; Pshenichnikov, M. S.; Bakker, H. J. Femtosecond Midinfrared Study of Aggregation Behavior in Aqueous Solutions of Amphiphilic Molecules. *J. Chem. Phys.* **2010,** *133*, 164514.

19. Di Michele, A.; Freda, M.; Onori, G.; Paolantoni, M.; Santucci, A.; Sassi, P. Modulation of Hydrophobic Effect by Cosolutes. *J. Phys. Chem. B* **2006,** *110*, 21077-21085.

20. Wilcox, D. S.; Rankin, B. M.; Ben-Amotz, D. Distinguishing Aggregation from Random Mixing in Aqueous T-Butyl Alcohol Solutions. *Faraday Disc.* **2013,** *167*, 177-190.

21. Comez, L.; Lupi, L.; Paolantoni, M.; Picchio, F.; Fioretto, D. Hydration Properties of Small Hydrophobic Molecules by Brillouin Light Scattering. *J. Chem. Phys.* **2012,** *137*.

22. Sinibaldi, R.; Casieri, C.; Melchionna, S.; Onori, G.; Segre, A. L.; Viel, S.; Mannina, L.; De Luca, F. The Role of Water Coordination in Binary Mixtures. A Study of Two Model Amphiphilic Molecules in Aqueous Solutions by Molecular Dynamics and Nmr. *J. Phys. Chem. B* **2006,** *110*, 8885-8892.

23. Fukasawa, T.; Tominaga, Y.; Wakisaka, A. Molecular Association in Binary Mixtures of Tert-Butyl Alcohol-Water and Tetrahydrofuran-Heavy Water Studied by Mass Spectrometry of Clusters from Liquid Droplets. *J. Phys. Chem. A* **2004,** *108*, 59-63.

24. Koga, Y.; Wong, T. Y. H.; Siu, W. W. Y. Vapor-Pressure of Aqueous Tert-Butanol in the Water-Rich Region - Transition in the Mixing Scheme. *Thermochimica Acta* **1990,** *169*, 27-38.

25. Shulgin, I. L.; Ruckenstein, E. Excess around a Central Molecule with Application to Binary Mixtures. *Phys. Chem. Chem. Phys.* **2008,** *10*, 1097-1105.

26. Koga, Y. Excess Partial Molar Enthalpies of Tert-Butanol in Water Tert-Butanol Mixtures. *Can. J. Chem.-Rev. Can. Chim.* **1988,** *66*, 1187-1193.

27. Clark, A. H.; Franks, F.; Pedley, M. D.; Reid, D. S. Solute Interactions in Dilute-Solutions .2. Statistical Mechanical Study of Hydrophobic Interaction. *Journal of the Chemical Society-Faraday Transactions I* **1977,** *73*, 290-305.

28. Omelyan, I.; Kovalenko, A.; Hirata, F. Compressibility of Tert-Butyl Alcohol-Water Mixtures: The Rism Theory. *Journal of Theoretical & Computational Chemistry* **2003,** *2*, 193-203.

29. Wilcox, D. S.; Rankin, B. M.; Ben-Amotz, D. Distinguishing Aggregation from Random Mixing in Aqueous T-Butyl Alcohol Solutions. *Faraday Discussions* **2013,** *167*, 177-190.

30. Bakulin, A. A.; Pshenichnikov, M. S.; Bakker, H. J.; Petersen, C. Hydrophobic Molecules Slow Down the Hydrogen-Bond Dynamics of Water. *J. Phys. Chem. A* **2011,** *115*, 1821-1829.

31. Lawton, W. H.; Sylvestre, E. A. Self Modeling Curve Resolution. *Technometrics* **1971,** *13*, 617-633.

32. Davis, J. G.; Gierszal, K. P.; Wang, P.; Ben-Amotz, D. Water Structural Transformation at Molecular Hydrophobic Interfaces. *Nature* **2012,** *491*, 582-585.

33. Davis, J. G.; Rankin, B. M.; Gierszal, K. P.; Ben-Amotz, D. On the Cooperative Formation of Non-Hydrogen Bonded Water at Molecular Hydrophobic Interfaces. *Nat. Chem.* **2013,** *5*, 796-802.

34. Fega, K. R.; Wilcox, D. S.; Ben-Amotz, D. Application of Raman Multivariate Curve Resolution to Solvation-Shell Spectroscopy. *Appl Spectrosc* **2012,** *66*, 282-8.

35. Ben-Amotz, D.; Herschbach, D. R. Estimation of Effective Diameters for Molecular Fluids. *J. Phys. Chem.* **1990,** *94*, 1038-47.

36. Tanaka, S. H.; Yoshihara, H. I.; Ho, A. W. C.; Lau, F. W.; Westh, P.; Koga, Y. Excess Partial Molar Enthalpies of Alkane-Mono-Ols in Aqueous Solutions. *Can. J. Chem.-Rev. Can. Chim.* **1996,** *74*, 713-721.

37. Raschke, T. M.; Tsai, J.; Levitt, M. Quantification of the Hydrophobic Interaction by Simulations of the Aggregation of Small Hydrophobic Solutes in Water. *Proc. Natl. Acad. Sci. U. S. A.* **2001,** *98*, 5965-5969.

38. Matsumoto, M. Four-Body Cooperativity in Hydrophonic Association of Methane. *J. Phys. Chem. Lett.* **2010,** *1*, 1552-1556.

39. Jacobson, L. C.; Hujo, W.; Molinero, V. Amorphous Precursors in the Nucleation of Clathrate Hydrates. *J. Am. Chem. Soc.* **2010,** *132*, 11806-11811.